Ultraviolet photolysis of acetaminophen in a 3D printed continuous flow reactor

by
John Goetze

A THESIS

submitted to

Oregon State University

Honors College

in partial fulfillment of
the requirements for the
degree of

Honors Baccalaureate of Science in Chemical Engineering
(Honors Scholar)

Presented May 29, 2019
Commencement June 2019

AN ABSTRACT OF THE THESIS OF

John Goetze for the degree of Honors Baccalaureate of Science in Chemical Engineering presented on May 29, 2015. Title: Ultraviolet photolysis of acetaminophen in a 3D printed continuous flow reactor

Abstract approved:_____

Nicholas AuYeung

Finding renewable sources of agricultural fertilizer will be necessary to ensure a stable food supply for future generations. Phosphorus is of particular concern, since mining phosphate rock is the main source and reserves are forecasted to deplete in the next 50 – 200 years. Human urine contains substantial amounts of nitrogen, phosphorus, and potassium. The value of urine as fertilizer is enhanced since the supply is nearly geographically ubiquitous, allowing for localized sourcing and treatment. Urine from the general population typically contains residual unmetabolized pharmaceuticals. Previous studies collected urine from human populations and found common pharmaceuticals on the order of tens to hundreds of micrograms per kilogram of urine, on average. Using urine as fertilizer for vegetables causes significant amounts of some drugs to be taken up into the edible parts of plants. Degradation of pharmaceuticals in human urine makes the urine a more feasible and accepted source of fertilizer. In this study, a 3D-printed miniature reactor which could be deployed in the field was created to demonstrate UV-degradation of pharmaceuticals. Possessing a well-characterized UV-visible spectrum, acetaminophen was the representative pharmaceutical selected for degradation in this study.

Batch and continuous flow reactors degraded acetaminophen using 254 nm artificial light. A continuous flow reactor was designed, 3D printed, and constructed. Acetaminophen photolysis was measured at an array of light intensities and flow rates through the reactor. Inlet concentrations of 2.5 and 5 ppm acetaminophen were tested. The amount of acetaminophen degraded through the reactor grew with increasing residence time and light intensity. Up to 80% of the acetaminophen was degraded in the continuous flow trials. Data was comparable to MFR and PFR models. These ideal models were fit to the data to determine pseudo-first order rate constants for photolysis.

Key Words: UV photolysis, 254 nm light, acetaminophen, pharmaceuticals in urine, 3D printing, microreactor

Corresponding e-mail address: goetzej@oregonstate.edu

Ultraviolet photolysis of acetaminophen in a 3D printed continuous flow reactor

by
John Goetze

A THESIS

submitted to

Oregon State University

Honors College

in partial fulfillment of
the requirements for the
degree of

Honors Baccalaureate of Science in Chemical Engineering
(Honors Scholar)

Presented May 29, 2019
Commencement June 2019

Honors Baccalaureate of Science in Chemical Engineering project of John Goetze presented on May 29, 2019.

APPROVED:

_____

Nicholas AuYeung, Mentor, representing Chemical Engineering

_____

Tyler Radniecki, Committee Member, representing Environmental Engineering

_____

Omar Mohamed, Committee Member, representing Chemical Engineering

_____

Toni Doolen, Dean, Oregon State University Honors College

I understand that my project will become part of the permanent collection of Oregon State University, Honors College. My signature below authorizes release of my project to any reader upon request.

_____

John Goetze, Author

Acknowledgements

I would like to thank the members of my committee for their individual contributions to my project. My mentor Dr. Nick AuYeung has been a tireless supporter of my learning and research for the past several years. He has provided innovative ideas and valuable feedback to maximize the impact of my efforts. Committee member Dr. Tyler Radniecki gave input on the feasibility of measuring degradation products and methods for the total organic carbon (TOC) analysis. Committee member Omar Mohamed, a doctoral student, provided resources for the knowledge of molecular orbital theory and photochemistry related this study. He also gave input on deciding the independent variables to test and equipment considerations for the 254 nm light source. In addition to my committee I am gracious to the Oregon State University Central Analytical Lab for assistance in obtaining TOC data.

The OSU School of Chemical, Biological, and Environmental Engineering has been instrumental in developing the abilities I needed to complete this investigation. The scientific background, application of engineering principles, and report writing skills developed during my education were all put to use for my thesis development. I also thank the Pete and Rosalie Johnson Foundation for selecting me and funding my research internship during summer 2015, which formed my original connection with Dr. AuYeung.

Lastly, I must thank my family and friends for their years of support for my academics and research. My parents Mike and Anne, and brother Peter consistently rekindle my interest in engineering and have encouraged me to engage deeply in the Honors College thesis experience. My partner Maddie and close friends have motivated me to work passionately in times of adversity and helped celebrate each milestone of success.

Table of Contents

Background 1
Human urine as fertilizer 1
Pharmaceuticals in urine 2
Ultraviolet photolysis of pharmaceuticals 3
Photolysis of acetaminophen 4
3D printing of chemical reactors 7
Experimental Methods 8
Source of acetaminophen and choice of concentrations for analysis 8
UV-vis spectroscopy 9
Ultraviolet light source 11
3D printed continuous flow reactor 12
Continuous flow trials 13
Batch studies and TOC measurement 15
Results and Discussion 16
Molar absorptivity 16
Batch photolysis, spectral analysis, and reaction products 17
Continuous flow photolysis 20
3D printed reactor performance 24
Conclusion 25
Further Research 25
Appendix A: Derivations 27
Appendix B: Supporting Figures 28
References 29

List of Figures

Figure 1: Molecular electronic excitations 3
Figure 2: Molecular structure of acetaminophen. 4
Figure 3: Solar spectrum mid-day in Corvallis, OR during sunny conditions 7
Figure 4: Warmup of UV-vis spectrometer measuring DI water 10
Figure 5: DL and LOQ for UV-vis spectrometer at wavelengths less than 400 nm 11
Figure 6: Spectrum of UV light source 12
Figure 7: 3D printed continuous flow reactor 13
Figure 8: Experimental apparatus for continuous flow trials 14
Figure 9: Linear relationship between UV-vis absorbance and unreacted acetaminophen concentration 16
Figure 10: Time dependent UV-vis spectral data for batch reaction 17
Figure 11: Total organic carbon analysis of photolysis products 19
Figure 12: Kinetic data of batch photolysis 20
Figure 13: Acetaminophen photolysis data in continuous flow reactor at varying intensities 21
Figure 14: SSE for ideal reactor model fits to continuous flow data 22
Figure 15: Relationship between UV light intensity and pseudo-first order rate constant (k') for MFR and PFR reactor models 22
Figure 16: Acetaminophen photolysis data incorperating UV light intensity and continuous flow reactor residence time 23
Figure 17: Relationship between UV light intensity and distance from light source 28
Figure 18: Calibration curve for syringe pump flow rate 28

List of Tables

Table 1: Concentration of selected drugs in general population sourced urine and drug concentrations in lettuce and soil after urine was added to field plots 2

Table 2: Compounds in Kroger acetaminophen tablet in descending order by mass 9

Table 3: Idealized reactor models from Levenspiel (1999)[38] 15

Table 4: Molar absorptivity of acetaminophen at 243 and 254 nm and comparison to literature 16

Table 5: Suggestion of primary photoproduct 18

Table 6: Pseudo-first order rate constants for a) MFR and b) PFR models at varied UV light intensities 22

Table 7: Ideal reactor performance equations considering UV-light intensity 23

Table 8: Pseudo-first order rate constants for MFR and PFR considering UV light intensity 24

Table of Nomenclature

Variable	Description	Units
E	Photon energy	J
h	Plank's constant	J-s
c	Speed of light	m/s
λ	Wavelength	nm
A	Time dependent UV-vis absorbance	Dimensionless
A_0	Initial UV-vis absorbance	Dimensionless
Φ	UV-vis light intensity	$\mu W/cm^2$
l	Distance UV-vis light passes through sample (arbitrary)	cm
d	Distance UV-vis light passes through sample (path length of equipment)	cm
C	Molar concentration	M = mol/L
ε	UV-vis molar absorptivity of analyte	$M^{-1}\ cm^{-1}$
$-r_A$	Instantaneous reaction rate	M/s
$\frac{dC_A}{dt}$	Instantaneous reaction rate	M/s
C_A	Time dependent reactant concentration	M
C_{A0}	Initial reactant concentration	M
I	Artificial light source intensity	W/m^2
τ	Continuous flow residence time or batch reaction time	min
k'	Pseudo-first order rate constant	min^{-1}
k	Pseudo-first order rate constant considering light intensity	$m^2/W\text{-}min$
n	Number of samples	Dimensionless, discrete
σ	Standard deviation	Data type dependent
X_A	Fractional conversion of reactant	Dimensionless

Background

Human urine as fertilizer

Human urine is a potential source of agricultural fertilizer but contains many pharmaceuticals that could pose an ecotoxicological risk. Fertilizers provide nitrogen, phosphorus, and potassium (NPK) to plants to promote growth and development. Human urine contains significant amounts of NPK in chemical forms that plants can utilize.[1, 2] Phosphorus is particularly important when considering urine as fertilizer. It is typically the growth-limiting nutrient in modern agriculture.[3] The global population is growing in magnitude and prosperity, demanding more calories per person as time goes on. This will substantially increase the need for phosphorus as fertilizer in the coming decades.

Phosphorus is obtained by either mining raw materials or recycling phosphorus available in the environment. Phosphorus in the environment only increases by human mining or the slow weathering of phosphorus rich rocks.[4] Multiple studies have assessed the remaining phosphorus available to be mined from the earth. These studies show that phosphorus reserves will likely be depleted in the next 50 – 200 years if current population trends continue.[4-7] Recycling of phosphorus in the environment will be necessary to grow food for future generations. In 2009 the global phosphorous available from human urine was 1.68 million metric tons, enough to satisfy around 10% of the global demand.[2] Nearly all phosphorous in urine is in soluble phosphate ions,[1] which are readily used by plants. Elemental phosphorus in urine ranges from 470 to 1070 mg/L.[1] Nitrogen in urine is mostly in urea and ammonia, which are not stable in long term aqueous storage at room temperature. Urea reacts with water to form ammonia, and ammonia vaporizes rapidly. Potassium in urine is mainly as K^+ ions in the range of 750 to 2610 mg/L.[1] The ions are valuable as fertilizer. Global potassium scarcity is of lower concern than phosphorus. Potassium is not commonly a rate limiting nutrient and is much more abundant in geological reserves.[7] Phosphorus is the most important of NPK when considering urine for its fertilizer value.

Source separation of urine maximizes its value for fertilizer. Obtaining phosphorus from wastewater is more difficult, as it is diluted and possibly contaminated with other materials auxiliary to those in urine. Widespread source separation in developed countries would require retrofitting of current sanitation facilities. Source separation could be implemented more easily in underdeveloped areas of the world that do not have modern sanitation facilities. New sanitation facilities could include the technology to segregate urine from other wastes. Coincidentally, many underdeveloped areas are in agricultural zones which suffer from a low supply of phosphorus; both from natural sources and lack of means to obtain fertilizer.[2] This increases the potential impact of source separation in new sanitation facilities to produce fertilizer from urine. Source separation of urine is also beneficial to reduce eutrophication.[4] The NPK would be kept out of wastewater, reducing unwanted algal blooms in fragile ecosystems.

Pharmaceuticals in urine

Widespread pharmaceutical use around the world has led to appreciable levels of these compounds in wastewater, posing an ecotoxicological risk. NSAIDs, antibiotics, and carbamazepine are consistently reported in the highest concentrations.[8-11] Pharmaceuticals are ingested by humans and metabolized in the body, then excreted in urine and feces. Metabolites are typically less ecotoxic than the parent drug, but there are many instances where metabolites pose a greater risk to aquatic life.[8] Despite the many metabolic pathways of pharmaceuticals, large portions of the parent drug pass through the body unmetabolized. Lienert et al. (2007)[8] assessed 42 pharmaceuticals for their metabolism in the human body, routes of excretion, and ecotoxicological potential in aquatic environments. An average of 50% of the parent drug was metabolized in the body, albeit with large variations among drugs. Most of the pharmaceutical and metabolite mass was excreted through urine, 70% on average. All but eight pharmaceuticals saw a decrease in ecotoxicity when metabolized. Acetaminophen showed an ecotoxicity risk in combination with its metabolites.

Mullen et al. (2015)[12] collected source separated urine from various public events in the United States and measured the concentrations of common drugs. The compounds found in the highest amounts are reported in Table 1 below. Field plots of lettuce were dosed with 1.7 L of urine per square meter of soil. The frequency of urine applications, and the time between application and harvest were not reported. Drug concentrations in soil and uptake by lettuce are given below. The acceptable daily intake (ADI) is the maximum amount of a drug that can be ingested by a person over a lifetime without any health consequences. ADI is expressed in µg of drug per kg of body weight per day and given by Snyder et al. (2008)[13] or Schwab et al. (2005).[14]

Table 1: *Concentration of selected drugs in general population sourced urine and drug concentrations in lettuce and soil after urine was added to field plots.*

Drug	Drug concentrations (µg/kg)[12]			Drug concentration ratio lettuce/soil	ADI (µg/kg/day)
	Urine	Lettuce	Soil		
Naproxen	310	3	35	9%	570[13]
Caffeine	525	9	61	15%	
Ibuprofen	120	9	38	23%	110[14]
Acetaminophen	510	7	12	63%	340[14]
Ciprofloxacin	200	3	2	200%	1.6[14]
Erythromycin	290	15	4	375%	40[14]
Carbamazepine	300	8	2	400%	0.34[13]

Carbamazepine, a psychoactive drug, poses the greatest risk to consumption in effective quantities from lettuce fertilized with urine. A 150 lb person must eat approximately 7 full heads of lettuce fertilized with urine to ingest the ADI of carbamazepine.

Wu et al. (2013)[15] also gauged the uptake of pharmaceuticals by vegetables. A hydroponics study was conducted by planting lettuce, cucumber, spinach, and peppers in an aqueous solution. The solution contained 20 common pharmaceuticals and personal care products in concentrations of 0.5 and 5 μg/L each. Plants were grown for 21 days in a greenhouse then analyzed. The ratio of drug concentration found in roots to that in the aqueous solution ranged from 10% to 100,000%. The same ratio for leaves ranged from 1% to 10,000%. Uptake of drugs by plants varied widely depending on each compound and type of plant. There is a wide distribution of results, but many instances of significant uptake shows that pharmaceuticals transferring to the vegetables is a legitimate concern. Wu et al. (2013)[15] used drug concentrations consistent with what is seen in wastewater. Concentrations in urine are two to three orders of magnitude greater than in wastewater, which would likely translate to much more uptake of the drugs into plants.

Ultraviolet photolysis of pharmaceuticals

The degradation of pharmaceuticals in urine and wastewater using UV light is an active area of research.[16-25] UV photolysis involves molecular level interactions between incident light with the electronic and vibrational energies of chemical bonds.[26-29] Regarding light, the relationship between the wavelength and photon energy is described by the equation below where E is the photon energy, λ is the wavelength, v is the frequency, h is Plank's constant, and c is the speed of light.

$$E = \frac{hc}{\lambda} = h\nu$$

A 254 nm monochromatic light source has individual and molar photon energies of 7.82×10^{-19} J and 4.71×10^{5} J/mol, respectively.

Molecules are described by translational, rotational, vibrational, and electronic energy.[28] Light incident on molecules can cause excitation of electrons. If the photon energy closely resembles the excitation energy of an electron, transitions to higher quantum states will occur.[29] Excitations typically proceed in valence electrons from non-bonding or bonding orbitals to antibonding orbitals, as seen in Figure 1 below.

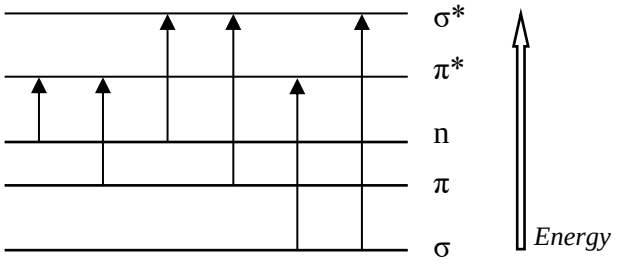

Figure 1*: Molecular electronic excitations from bonding (σ, π) and non-bonding (n) to antibonding (σ*, π*) states. Adapted from Reusch (2013b).*[25]

The transition of an electron to an antibonding orbital alters the potential energy of repulsion between the nuclei in a bond. The new minimum in the potential energy curve occurs at a greater distance between nuclei, causing an excitation in the vibrational state of the bond.[28] The Franck-Condon principle states that the electronic excitation occurs much faster than the vibrational state transition.[28] If the photon absorption raises the vibrational energy higher than the dissociation energy of the bond, cleavage may occur.[28] In this case, two new radical species are formed. If the vibrational state is excited less than the bond dissociation energy, the electron will return to its ground state, and the vibrational state will follow.[26] During electron relaxation a single photon may be emitted via fluorescence, multiple different photons may slowly be emitted as the electron steps down through many quantum states via phosphorescence, or the energy may be lost as heat through radiative decay.[26]

The energy required to excite valence electrons in a bond is related to the bond conjugation.[27] Conjugation occurs in systems of alternating single and double bonds when π bonding orbitals and non-bonding p orbitals overlap (conjugate).[27] The more conjugated a system, the lower the energy of excitation for valence electrons.[27] Pharmaceuticals are often large molecules that contain phenyl rings and many double bonds in close proximity. The high prevalence of such structures means that most pharmaceuticals can absorb wavelengths in the 100 – 400 nm (ultraviolet) range.

Photolysis of acetaminophen

The U.S. pharmaceutical industry was worth $333 billion in 2016.[30] Thousands of different drugs are purchased over-the-counter and prescribed by doctors. Each drug is different in its prevalence in society, metabolism, route of excretion, and ecotoxicity. Acetaminophen (also known as paracetamol) is a widely used NSAID pain reliever and is the object of this study for several reasons. It is consistently measured in relatively high concentrations in municipal wastewater,[8-11] is easily obtained over-the-counter, and concentration can be measured with ultraviolet-visible spectroscopy (UV-vis). Albeit the structure of acetaminophen (shown below in Figure 2) is relatively simple compared to some other pharmaceuticals, it contains bonds that can absorb UV light.

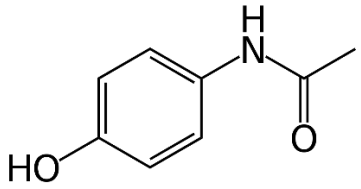

Figure 2: *Molecular structure of acetaminophen.*

Acetaminophen exhibits a strong UV-vis peak at 243 nm and behaves in agreement with the Beer-Lambert law.[31-34] The Beer-Lambert law states that UV-vis absorption scales linearly with concentration of the analyte.[27, 29, 35] UV-vis absorption is also called extinction because it measures the decrease in light intensity through a solution of analyte.[27, 29] Absorption in UV-vis

spectroscopy is attenuation; produced by both photon absorption and light scattering.[29] It is dimensionless and defined by the equation below[29] where A is absorbance and $\Phi(\lambda,l)$ is the intensity of wavelength λ at distance l through the sample. The distance the light passes through a sample solution, known as the path length, is d.

$$A = \log\left[\frac{\Phi(\lambda,0)}{\Phi(\lambda,d)}\right]$$

UV-vis spectroscopy is possible because molecules attenuate light at different magnitudes depending on the wavelength.[35] The range normally tested is from 200 – 1100 nm.[35] The varying attenuation at each distinct wavelength produces a unique spectrum for each compound. Molecular structure determines spectrum shape, and concentration determines the relative absorbance of each peak.[35] The molar absorptivity (ε), is an intensive property defined at individual wavelengths. It relates the absorbance (A), molarity (C), and path length (l), as shown below. [27, 29, 35] The units of ε are $M^{-1}\,cm^{-1}$.

$$\varepsilon = \frac{A}{Cl}$$

Multiple batch reactor studies have irradiated acetaminophen with UV light to induce photolysis, and report time dependent UV-vis data.[31, 34, 36, 37] Time dependent absorbance data for a single wavelength (e.g. 243 nm) is typically expressed as a ratio (A/A_0) with respect to the initial absorbance (A_0). Nearly all applicable literature models acetaminophen photolysis with pseudo-first order kinetics. This kinetic model only considers the rate of disappearance of acetaminophen and not any of the photolysis products. The pseudo-first order rate law is shown below, which includes the instantaneous reaction rate ($-r_A$), lumped rate constant (k'), and instantaneous acetaminophen concentration (C_A). The constant k' is in units of min^{-1} and is denoted k' instead of k because it does not consider light intensity.

$$-r_A = \frac{dC_A}{dt} = k'\,C_A$$

Levenspiel (1999)[38] provides the performance equation for pseudo-first order kinetics in a batch reactor. The equation additionally considers the duration of the reaction (τ) and initial acetaminophen concentration (C_{A0}) and is shown below. The Beer-Lambert law affirms that C/C_0 equals A/A_0.

$$-\ln\left[\frac{C_A}{C_{A0}}\right] = -\ln\left[\frac{A}{A_0}\right] = k'\tau$$

Rate constants are reported in literature but vary widely based on the type and intensity of light used. Xu et al. (2018)[32] used 254 nm light of 3.2×10^{-6} Einstein/s to degrade aqueous acetaminophen in initial concentrations of 0.8 – 6 ppm. The pseudo-first order rate constant was

k' = 1.2 –1.3 x 10^{-3} min^{-1} for all trials. Carlson et al. (2015)[33] used 254 nm light at 1.4 W/m^2 with 50 ppb acetaminophen and reported k' = 2.04 x 10^{-3} min^{-1}.

Photolysis reactions produce products. In the case of acetaminophen, multiple studies have proposed photolysis products depending on the wavelength of irradiated light and conditions in the reactor. Pozdnyakov et al. (2014)[36] irradiated aqueous acetaminophen with 254, 266, and 282 nm monochromatic light. Time dependent UV-vis spectra were shown for each wavelength. HPLC–MS was used to identify seven photoproducts, all of which had eight or more carbon atoms per molecule. Unreacted acetaminophen is an eight carbon molecule. Major and minor photoproducts were given for irradiance at each separate wavelength. Martignac et al. (2013)[37] irradiated acetaminophen with 254 nm light and proposed multistep reaction mechanisms in argon and oxygen saturated solutions. HPLC was used for the analysis. Photoproducts in the oxygen saturated solution all had a greater molecular weight than acetaminophen. Kawabata et al. (2012)[39] irradiated acetaminophen with 254 nm light and identified a single major photoproduct, which was an isomer of acetaminophen. This isomer proved to be more ecotoxic than acetaminophen in a bioluminescent bacteria test. In this test bioluminescent bacteria are exposed to compounds of interest. The intensity of light they emit determines the amount of stress the compound placed on the bacterial population. Literature provides many possible products of acetaminophen photolysis. There is conflicting information on the exact identity of these products, but the majority are the same or greater molecular weight than acetaminophen.

The sun was the source of UV light for the first scientific investigations of photochemistry. Giacomo Ciamician from the University of Bologna used sunlight to reduce quinone to quinol in 1886[26] and, thus, the field of photochemistry was born. Sunlight provides highest intensity light in the visible (400 – 740 nm) range. Shorter wavelengths in the UV-A (315 – 400 nm) range have higher photon energy, but the solar intensity is less than in the visible range. Looking at even shorter wavelengths, sunlight provides some radiation in the UV-B (280 – 315 nm) range, and a negligible amount in the UV-C (100 – 280 nm) range. A solar spectrum is shown in Figure 3 below.

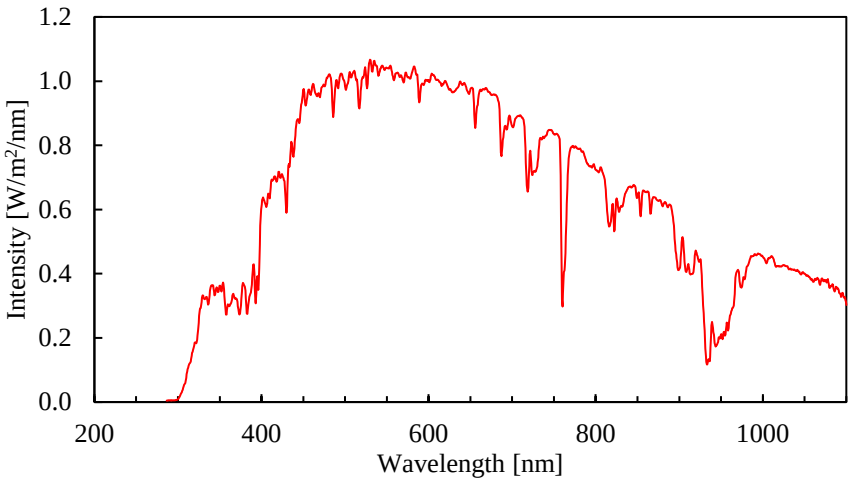

Figure 3*: Solar spectrum mid-day in Corvallis, OR during sunny conditions, May 2017. Measurement methods are detailed in the experimental methods section.*

Most research into the photolysis of pharmaceuticals uses artificial UV light in the range of 254 – 365 nm. Higher energy (shorter wavelength) light is generally more successful for drug degradation. The drop off in solar intensity below 400 nm creates limitations for pharmaceutical photolysis. The feasibility of acetaminophen photolysis using sunlight has been studied and shown mixed results. Kawabata et al. (2013)[40] irradiated aqueous acetaminophen with 254, 302, and 365 nm artificial light and unconcentrated sunlight. Degradation of acetaminophen was only observed with the 254 nm artificial light. In contrast, Mujahid et al. (2014)[31] and Eskandarian et al. (2016)[34] both degraded acetaminophen using artificial light at 365 nm. The 365 nm light is well within the range where the sun provides substantial radiation. It is conceivable that concentrated solar radiation could degrade acetaminophen by providing high enough intensity in the UV-A range. The broad spectrum of sunlight may produce different photolysis products than previous studies[36, 37, 39] using artificial light because the artificial light is typically monochromatic. Sunlight could have advantages over artificial light, depending on the degree of concentration required to achieve photolysis. Capital requirements, operating costs, and feasibility in remote areas would likely determine this advantage.

3D printing of chemical reactors

3D printing is gaining popularity in research and industry. It streamlines the construction of prototypes and production of specialized components in small volumes.[41, 42] Take, for example, a protective case for a smart phone. The traditional process for creating a prototype requires a stock material to be machined or formed to precise dimensions. If the prototype is moved to larger scale production precise molds must be created for an injection molding process. A large amount of time and resources is required to create a prototype and develop a mold of a part for production.[42] The investment required is such that large production volumes are often required to turn a profit.[42] 3D printing requires far less time and resources to build individual prototypes because the need for machining is ideally eliminated.[41] A CAD model is sent to the printer, which automatically creates the part exactly as specified. 3D printing is typically

economic in small volumes compared to injection molding because the startup cost for each new part is much less.[41]

There are two types of 3D printers widely in use today.[42] Fused deposition modeling (FDM) printers extrude a thermoplastic through a nozzle, building up a part layer on top of layer like frosting on a cake. FDM printers typically appeal to the consumer market and are limited in precision and printable materials.[42] Acrylonitrile butadiene styrene (ABS) and polylactic acid (PLA) are the most common thermoplastics used. FDM printers can only build a component by progressing in the upward direction. Parts with overhang in a lateral direction require supports. Selective laser sintering (SLS) printers provide many advantages to FDM printers. SLS printers use a powder bed of plastic or plastic and metal. A laser sinters a pattern in the powder bed corresponding to the individual layer of the part being printed. Layer by layer, the 3D printed part is sintered together from the powder bed. Parts extending laterally with an overhang can easily be printed with SLS because the un-sintered powder acts as an inherent support structure. The powder that is not sintered is blown away after printing is complete, revealing a solid part. SLS is typically more capital intensive than FDM but offers much greater precision and eliminates the need for supports during printing.[42]

3D printing is becoming more common in chemical engineering research. Stefanov et al. (2015)[43] created a 3D printed reactor for gas phase analysis of photocatalytic reactions in continuous flow. Lopes et al. (2019)[44] created a micro-scale biodiesel plant using 3D printed components. The micro-plant produced 125 mL/min of biodiesel and offered valuable data for the potential scale up of the process. Zhao et al. (2018)[45] used 3D printing in the development of luminescent solar concentrator photo-microreactors. The study rapidly produced many different prototypes and offered a method for scaling up the process by numbering up the reactors. 3D printing is proving its worth in research and manufacturing applications due to rapid fabrication of specialized components. It eliminates the constraints of using only standardized parts and of doing time-consuming forming and machining.[42] The ability for specialized components to be created quickly allows researchers and manufacturers to speed development of new technologies.

Experimental Methods

Source of acetaminophen and choice of concentrations for analysis

Acetaminophen was obtained from Kroger 500 mg acetaminophen caplets intended for therapeutic use. Preparation of aqueous acetaminophen was done by crushing a single tablet and mixing with 500 mL of deionized water (DI) to create a 1000 ppm solution. The 1000 ppm solution was stirred and heated to aid the dissolving of acetaminophen from the solid tablet. The solution was heated from room temperature to 60 ^{o}C in a span of 10 minutes, then maintained at 60 ^{o}C for an additional 15 minutes. Vigorous stirring with a magnetic stir bar was done continuously throughout the 25 minute heating process. The 1000 ppm solution was diluted in two steps to the final concentrations for analysis. Aqueous acetaminophen was kept in beakers covered with Parafilm. A sample of 10 ppm acetaminophen was stored for 14 days and showed

no measurable degradation over the entire time span, via UV-vis analysis. Despite this, solutions were remade after no more than three days of storage in case of any solvent evaporation.

The acetaminophen tablets contained supplementary inactive ingredients. Tablets weighed 555.8 mg on average ($n = 75$, $\sigma = 5.0$). The inactive ingredients added an additional 11% of mass in solution with respect to the acetaminophen and are listed below in Table 2.

Table 2: *Compounds in Kroger acetaminophen tablet in descending order by mass.*

Compound	Mass in tablet
Acetaminophen	500 mg
Carnauba wax Corn starch Croscarmellose sodium Hypromellose Polyethylene glycol Povidone Pregelatinized starch Sodium starch Glycolate Stearic acid	Sum of inactive ingredients: 55.8 mg

The aqueous acetaminophen concentrations used in this study are 2.5 ppm and 5.0 ppm. Concentration is measured by the UV-vis absorbance at 243 nm. The limit of quantitation (LOQ) at 243 nm for the UV-vis spectrometer is 0.0094 in units of absorbance, computed with the method defined by Harris (2016).[35] Acetaminophen at 2.5 ppm can be degraded to 4.8% of its original concentration before the absorbance peak is reduced below the LOQ. Human urine collected from public events has been measured to contain 0.5 ppm acetaminophen by Mullen et al. (2015).[12] Analysis of 2.5 ppm acetaminophen was chosen because the degradation can be well studied above the LOQ and it is within one order of magnitude of the concentration in urine. Varying the concentration to be degraded is useful for a kinetic analysis. Worldwide acetaminophen concentrations in urine are likely far from uniform, giving additional reason to test multiple levels. A high concentration of 5 ppm was studied in addition to the low concentration of 2.5 ppm.

UV-vis spectroscopy

Ultraviolet-visible spectroscopy was done using an Avantes AvaSpec-ULS204BCL-EVO multiplex detector equipped with an AvaLight-DHc light source. The DHc light source had a deuterium light and a halogen light. The range of wavelengths emitted was 200 – 400 nm for deuterium, and 400 – 2500 nm for halogen, as stated by the manufacturer. Both the deuterium and halogen light were used. The sample was analyzed with an Avantes Micro flow Z-cell-10 with an optical path length of 1.0 cm. A reference spectrum for DI water was measured and saved into the spectrometer software (AvaSoft 8.7.1) as well as a dark reference spectrum. New reference spectrums were taken at least once a day after the spectrometer had warmed up. The

reference spectrums allow the spectrometer to distinguish the analyte absorbance from the solvent.

The UV-vis spectrum often exhibited a baseline shift during experimental trials. The shift was corrected by normalizing the spectrum to the measured absorbance at 390 nm. The entire acetaminophen peak was contained in wavelengths less than 310 nm, and the deuterium light source provided wavelengths up to 400 nm. Correction was done at 390 nm because it is far from the acetaminophen peak and is unaffected by the transition between the deuterium and the halogen light ranges.

The warmup time of the spectrometer was gauged. DI water was pumped through the flow cell for 30 minutes at 35 µL/min and the absorbance spectrum was measured each minute, as shown in Figure 4. A reference spectrum for the DI water was not recorded before or during the warmup, explaining the deviation of absorbances from near-zero. Recording a reference spectrum sets all wavelengths to an absorbance of zero. The spectra were not corrected for the baseline shift.

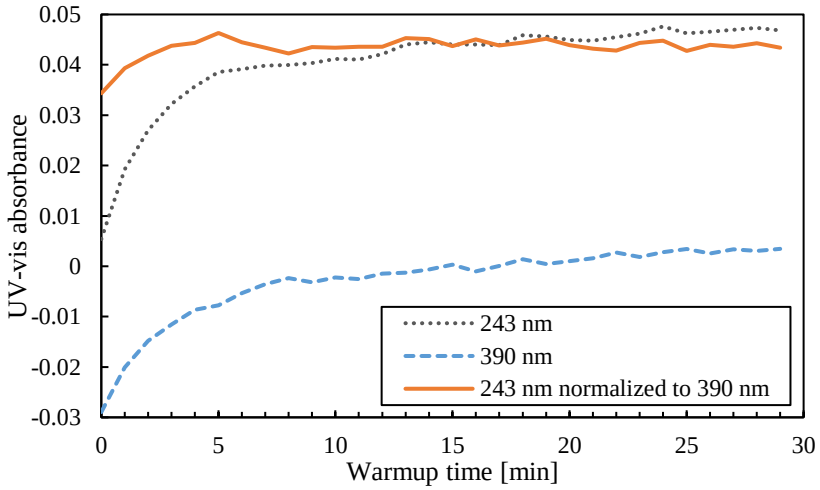

Figure 4: *Warmup of UV-vis spectrometer measuring DI water. A reference spectrum was not recorded, nor were spectra corrected. 243 nm and 390 nm are shown, representing the acetaminophen peak and the baseline correction wavelength, respectively.*

The spectrometer exhibits exponential warmup in the first 5 minutes, then a slow and sustained growth in measured absorbance after 5 minutes. The difference between absorbances at 243 and 390 nm is stable after 5 minutes. The lack of an upward or downward trend in the difference indicates that 390 nm is a good choice for normalizing the UV-vis baseline, in the interest of measurement at 243 nm.

The LOQ for the spectrometer was determined from a separate trial. The spectrometer was warmed up for 45 minutes, then DI water was pumped through the flow cell at 35 µL/min. The spectrum was measured every minute for 30 minutes. Each spectrum was normalized to 390 nm to account for baseline shift. A standard deviation (S) was computed for measurement at each wavelength. The detection limit (DL) and LOQ for each wavelength were expressed as 3S and

10S, respectively, based on Harris (2016).[35] The LOQ for absorbance at 243 nm is 0.0094, as stated previously. Figure 5 below shows the LOQ and DL graphically for each wavelength.

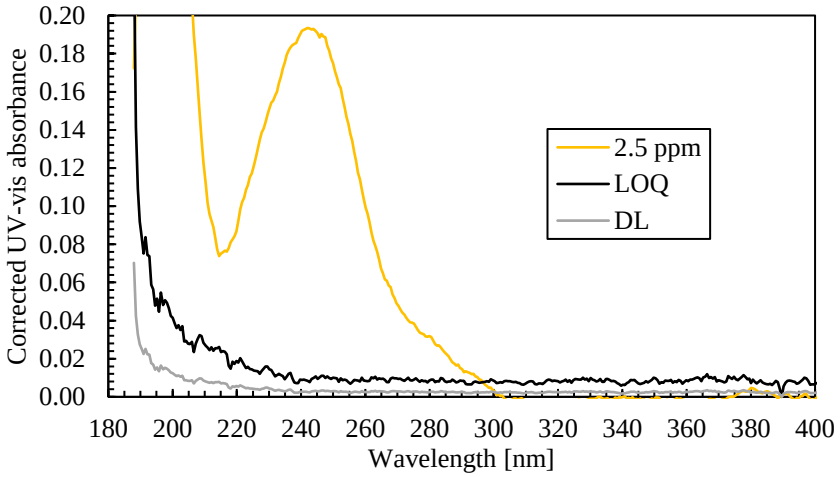

Figure 5: *DL and LOQ for UV-vis spectrometer at wavelengths less than 400 nm. 2.5 ppm acetaminophen spectrum shown for reference of scale.*

Measurement of the solar and 254 nm artificial light source spectra was done using the multiplex detector in the UV-vis spectrometer equipped with an Avantes CC-UV/VIS cosine corrector to capture incident light. The spectrometer was switched from absorbance mode to absolute irradiance mode. Only a dark reference was needed in order to measure the spectra of the sun and the 254 nm light. The measured solar spectrum is shown in Figure 3 above. Integrating the spectrum yields a total solar intensity of 524 W/m^2.

Ultraviolet light source

The artificial light source used was an Aqua Ultraviolet Classic 80-Watt Sterilizer. It has a low pressure mercury lamp rated to produce monochromatic light at 254 nm. Light was measured to emit a sharp peak between 251 – 255 nm with a lambda max of 252.9 nm. The UV light is referred to as the 254 nm light to keep consistent with literature and since the intensity at 254 nm is still significant, as seen in Figure 6a. Other emission peaks were measured but none were comparable to the 254 nm peak, as seen in Figure 6b. The light was kept powered on continuously to avoid any effects of warmup.

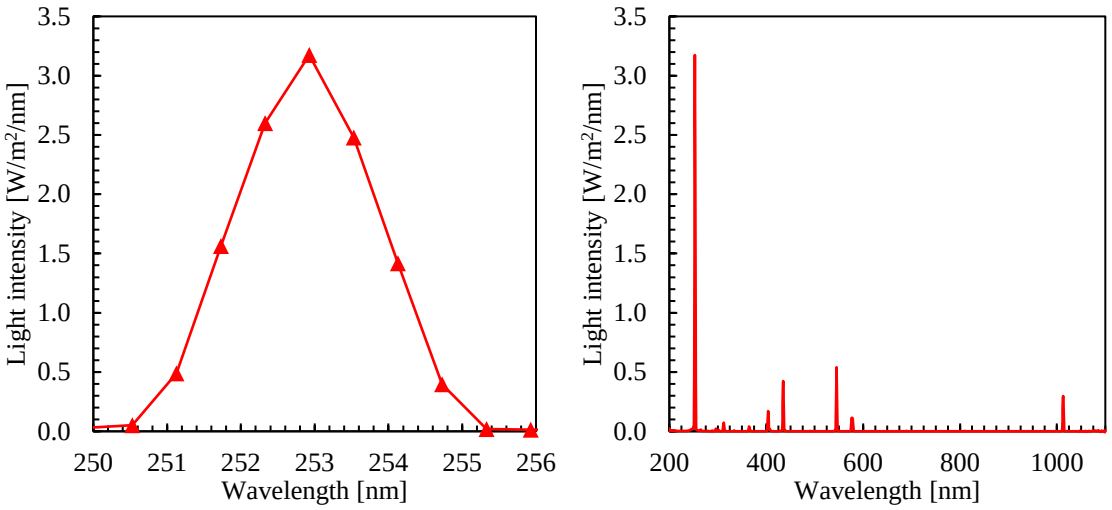

Figure 6: *Spectrum of UV light source. a) Focused view of intensity near 254 nm. b) Full UV-vis spectrum.*

3D printed continuous flow reactor

The continuous flow reactor was constructed of many components, most of which were 3D printed. The design and construction are shown visually in Figure 7 below. The region of the reactor where UV light irradiated acetaminophen was 19 mm in diameter and 6 mm deep, giving a total volume of 1701 µL (1.7 mL). SOLIDWORKS 2018 was the platform for CAD modeling of the reactor. The 3D printer was a MakerBot Replicator 2 FDM printer using PLA plastic for extrusion. A total of nine unique components were 3D printed, as shown in Figure 7a below.

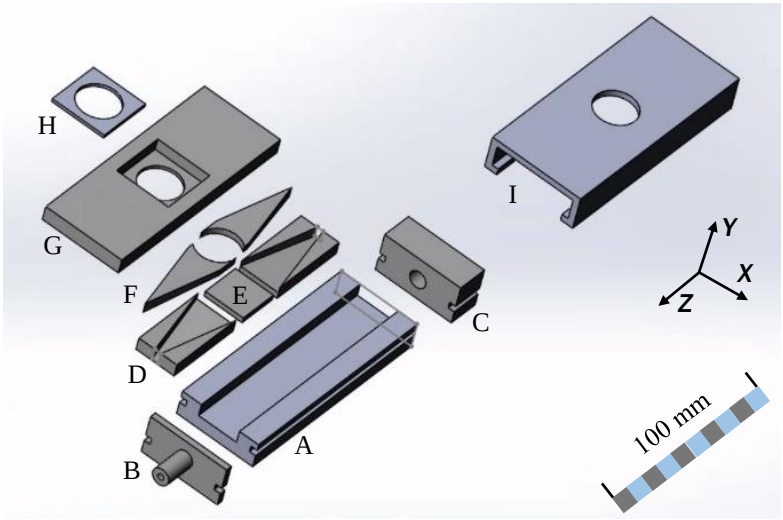

a)

b)

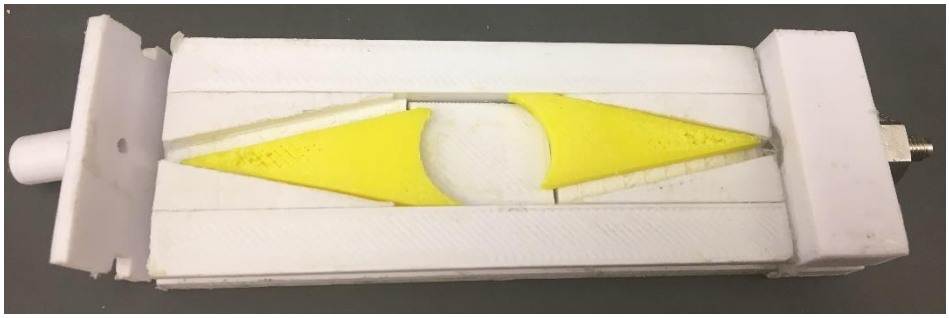

c)

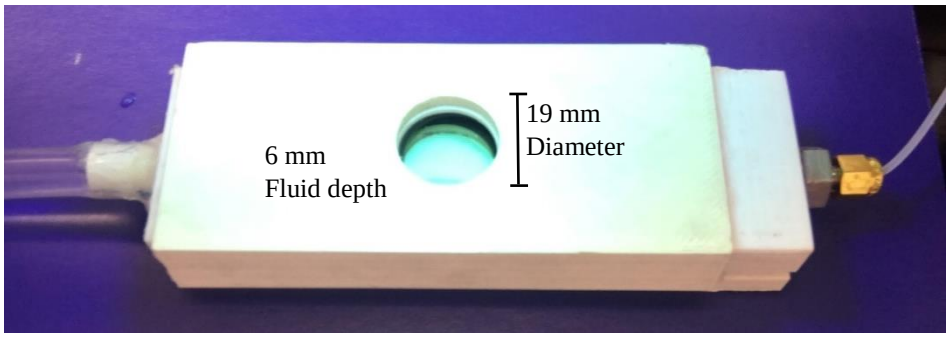

Figure 7: *3D printed continuous flow reactor. a) SOLIDWORKS exploded model of 3D printed components, including part labels. b) Partially constructed reactor showing fluid flow channel. c) Fully constructed and functioning reactor during an acetaminophen photolysis trial.*

All parts were printed with 66% infill of PLA except for parts C and I, which were printed with 100% infill. Part C was drilled and tapped so that a Swagelok fitting could be secured to the reactor outlet, as seen in Figure 7c. In part I, the hole shown was drilled after the part was printed since the FDM printer could only print in one direction (z dimension in this case) without any voids or overhang. Parts D, E, and F fit into part A to form the flow channel, as shown in Figure 7b. Parts B and C provide the reactor inlet and outlet connections. Between parts G and H are a thin glass slide and two O-rings, which can be seen in Figure 7c. The subassembly of part G, the glass slide, O-rings, and part H is placed on top of part A. Part I fits into the grooves in part A and is slid across in the z direction to form the top of the reactor. The close fit of part I exerts a downward force on part H, forming a pressure seal between the glass slide, O-rings, and part G. Silicone caulk and superglue were used to bond components together and seal leak points throughout the reactor. The glass slide was made of single crystal sapphire and sourced from AdValue Technology. Single crystal sapphire was chosen because of its low attenuation of UV light; 30 – 35% at 254 nm as stated by the manufacturer.

Continuous flow trials

Aqueous acetaminophen was degraded with UV light in the continuous flow reactor while varying the initial concentration, flow rate, and light intensity. Initial concentrations of 2.5 ppm and 5 ppm were analyzed, as mentioned previously. Flow rates tested were 10, 15, 25, 35, 75, and 100 μL/min. The intensity of UV light was varied by changing the distance of the reactor from the light source. The distance from the rim of the light down to the flowing acetaminophen was 10 mm when the top of the reactor was positioned flush with the rim, as shown in Figure 8 below.

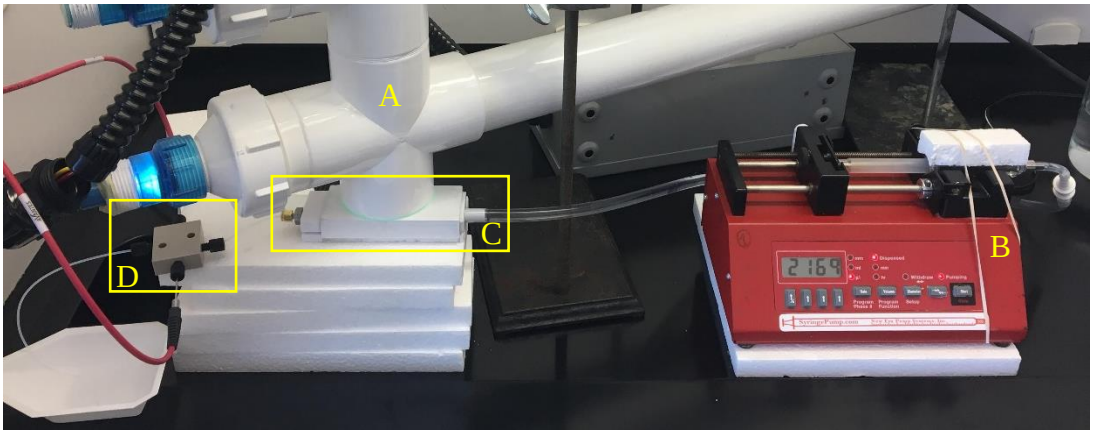

Figure 8: *Experimental apparatus for continuous flow trials. Equipment includes 254 nm light source (A), syringe pump (B), 3D printed reactor (C), and UV-vis flow cell (D).*

The 10 mm distance from the rim of the light to the flowing acetaminophen was increased to 50 and 90 mm to change the light intensity. The distance was controlled by varying the height of the reactor above the benchtop. The UV light intensity (integration from 251 – 255 nm) was measured at each distance. A spare single crystal sapphire slide was placed over the detector to simulate experimental conditions. The intensities at each distance were 20.31, 9.09, and 5.07 W/m^2. Detailed graphical data for dependence of UV light intensity on distance, measured every 10 mm, is shown in Figure 17 in the appendix.

Fluid flow was provided by a New Era Pump Systems NE-1000 syringe pump. The syringe pump flow rate was programable so long as the syringe diameter was known. Actual flow rate was gauged by measuring the mass of fluid discharged from the UV-vis flow cell over a set amount of time. Flow rate data was gathered across all three reactor heights (light intensities) for each flow setting. The data confirms the accuracy of the syringe pump flow settings and is shown graphically in Figure 18 in the appendix.

All 5 ppm trials were completed first and randomized with respect to flow rate and light intensity. Trials for 2.5 ppm were completed next and randomized in the same respect. Replicate trials were not completed due to time constraints. The UV-vis absorbance was measured at the beginning of each trial with unreacted acetaminophen flowing in the reactor. The reactor was then put under the 254 nm light and UV-vis absorbance measured until steady state was reached, which was at least three times the residence time for each trial. Steady state conditions were verified by ensuring the absorbance was unchanged for at least 20 minutes for 75 and 100 µL/min flows, and at least 45 minutes for flows 35 µL/min and less.

Kinetic analysis of the acetaminophen degradation was done utilizing two idealized reactor models. Levenspiel (1999)[38] defines an ideal mixed flow reactor (MFR) and plug flow reactor (PFR) using the assumptions and performance equations shown in Table 3 below. Fractional conversion (X_A) is equal to one minus A/A_0 for the purposes of this study. Recall that the Beer-Lambert law states that C/C_0 equals A/A_0.

Table 3: *Idealized reactor models from Levenspiel (1999).*[38]

Idealized reactor model	MFR	PFR
First order reaction performance equation	$k'\tau = \frac{X_A}{1-X_A}$	$k'\tau = \ln\left[\frac{1}{1-X_A}\right]$
Key assumptions	- Reactor is well mixed so that concentration is uniform throughout working volume.	- Reaction progresses as fluid moves unidirectionally through reactor. - Concentration is uniform through the cross section perpendicular to flow.

Batch studies and TOC measurement

A batch reaction was completed to compare spectral and kinetic data with the continuous flow reactor. The batch reactor was an open beaker containing 25 mL of liquid at a depth of 6 mm, the same depth as the fluid in the continuous flow reactor. The acetaminophen concentration was increased to 10 ppm. The surface of the liquid was 3 mm from the rim of the UV light and the intensity was 23.83 W/m^2. The solution was stirred constantly with a magnetic stir bar. UV-vis data of batch trials was measured every ten minutes using cuvettes instead of the flow cell. The cuvettes were Fisherbrand Macro Optical Quartz with a 1.0 cm path length. A new DI reference and dark reference were recorded into the spectrometer before each measurement of the batch data.

Total organic carbon (TOC) was measured to give insight on the photolysis products of acetaminophen. Complete degradation, also called mineralization, converts acetaminophen to CO_2. CO_2 is considered inorganic carbon. Photolysis products may be organic molecules or CO_2. The TOC instrument used was a Shimadzu TOC-VCSH, which uses the combustion oxidation method. Analysis required 45 mL samples. Batch trials were completed because of the prohibitively long time to produce 45 mL of sample through the continuous flow reactor, since flow rates were on the order of microliters per minute. Batch trials for TOC were done in an open beaker containing 50 mL of aqueous acetaminophen at a liquid depth of 11 mm. The surface of the liquid was approximately 5 mm from the rim of the UV light yielding a light intensity of 22.96 W/m^2. The solution was mixed constantly with a magnetic stir bar. An initial acetaminophen concentration of 10 ppm was used so that the organic carbon levels would stay above the LOQ of the TOC instrument. The solution was filtered with a 0.20 μm tolerance to remove any of the inactive ingredients from the acetaminophen tablet before irradiation. All but one of the inactive ingredients contain long carbon chains or are polymers, which would have been removed by the 0.20 μm filter. Samples were tested of filtered 10 ppm acetaminophen irradiated for different durations. A first group was irradiated until UV-vis absorbance reached A/A_0 = 30 – 40%. A second group to A/A_0 < 10%. A control group was not irradiated. Two trials were completed for each group.

Results and Discussion

Molar absorptivity

The UV-vis spectrum was measured in the flow cell with unreacted acetaminophen concentrations of 1.0, 2.5, 5.0, 7.5, 10.0, and 12.5 ppm. Graphical results are shown below in Figure 9. The lambda max was confirmed to be 243 nm. Absorbance at the 243 nm peak and at 254 nm were compared to literature.

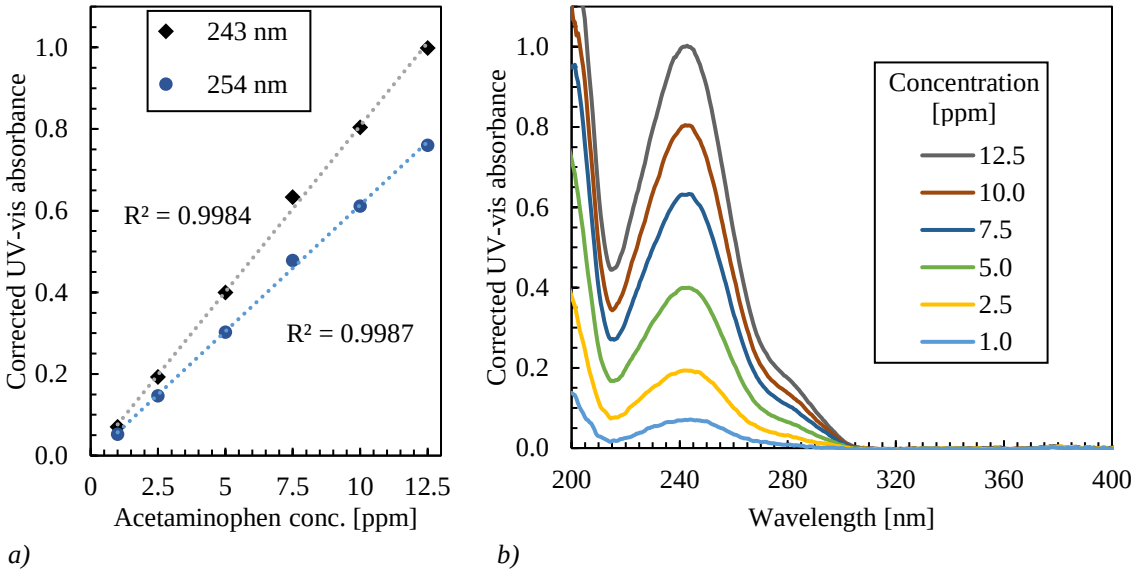

Figure 9: *Linear relationship between UV-vis absorbance and unreacted acetaminophen concentration. a) 243 and 254 nm absorbance vs concentration with linear fit shown. b) UV-vis spectra at different concentrations.*

The excellent fit of the data confirms the Beer-Lambert law is valid in the given concentration range with the UV-vis spectrometer and flow cell in this study. The molar absorptivity was determined to be ε = 12,203 ± 309 L mol^{-1}cm^{-1} (95% CI) at the absorption peak of 243 nm and ε = 9271 ± 213 L mol^{-1}cm^{-1} (95% CI) at 254 nm. The molar absorptivity agrees with previous studies that have used a pure acetaminophen reagent, as shown in Table 4 below.

Table 4: *Molar absorptivity of acetaminophen at 243 and 254 nm and comparison to literature. Confidence interval shown for this study is 95%.*

Source	ε_{243} [L mol^{-1}cm^{-1}]	Source	ε_{254} [L mol^{-1}cm^{-1}]
Kawabata et al. (2013)[40]	13,705	Carlson et al. (2015)[33]	7800
		Martignac et al. (2013)[37]	9680
This study	12,203 ± 309	This study	9271 ± 213

Consistency in molar absorptivity with literature validates the methods for obtaining accurate amounts of acetaminophen, and the methods of operation for the UV-vis spectrometer. All the acetaminophen dissolved from the Kroger 500 mg tablet. Concentration was able to be measured accurately and repeatably with the spectrometer.

Batch photolysis, spectral analysis, and reaction products

The batch reactions yielded UV-vis spectra for that give insight to the photolysis reaction products. The spectra changed shape with increased photolysis in the same way for both the batch and continuous flow reactors. This suggests that each reactor is producing the same photolysis products in the same kinetic ratios. The UV-vis spectra can be used from either reactor to examine the possible reaction products. Figure 10 below shows how the spectra change as the reaction progresses.

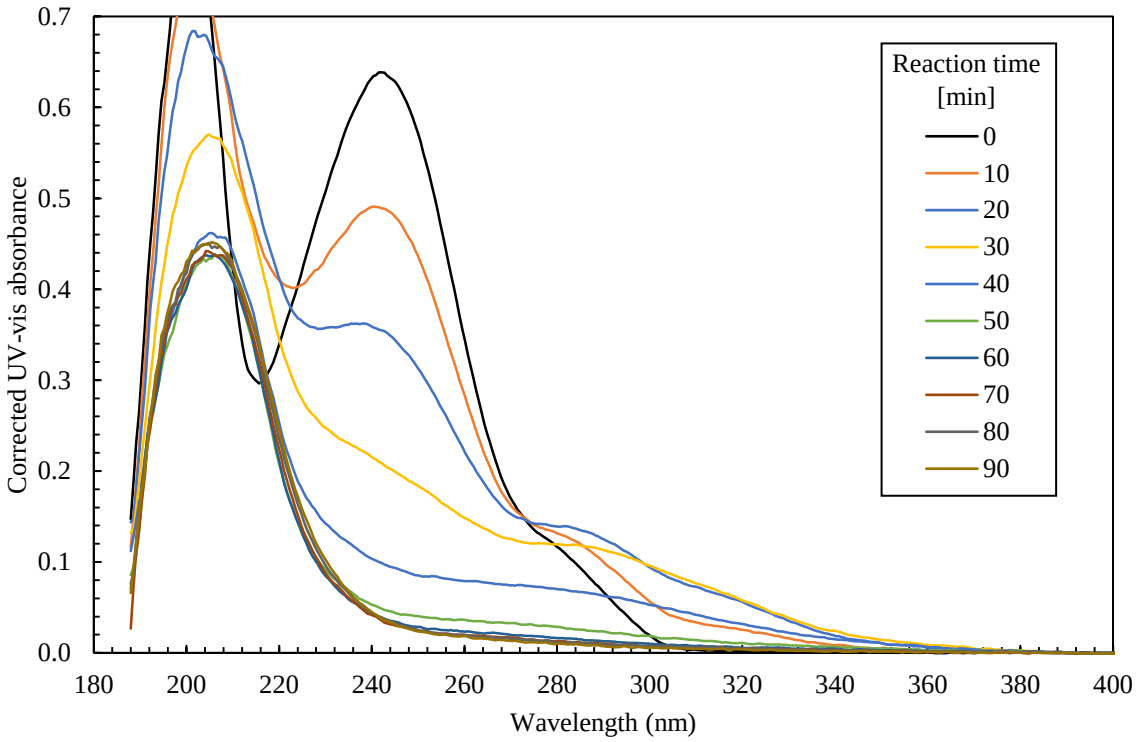

Figure 10: *Time dependent UV-vis spectral data for batch reaction.*

The spectral data suggests two phases of the reaction. In the first phase (0 – 20 min) the 243 nm peak is reduced in magnitude and the peak location is unchanged. A secondary peak near 285 nm grows in magnitude during the first phase of the reaction. This suggests the appearance of a new and different organic molecule with conjugated bonds that absorb in the UV region. In the second phase of the reaction (30 – 60 min) the absorbance decays nearly uniformly across the entire spectrum, suggesting disappearance of both acetaminophen and the organic photoproduct created during phase one. Beyond 60 minutes the spectrum does not change significantly, meaning the reaction has stopped. The peak near 207 nm persists, suggesting the existence of a separate organic photoproduct that does not degrade in the UV irradiance conditions.

Pozdnyakov et al. (2014)[36] degraded aqueous acetaminophen with UV light at 254, 266, and 282 nm and provided a UV-vis and HPLC-MS analysis of photoproducts. The UV-vis spectral results for degradation with 266 nm light matched the spectral results of this study, yet

the 254 and 282 nm trials were distinctly different. Specific comparisons are shown in Table 5 below.

Table 5: *Suggestion of primary photoproduct based on consistencies with Pozdnyakov et al. (2014).*[36]

Irradiation wavelength	**Primary photoproduct**	**UV-vis spectral characteristics**	**Comparison to UV-vis results in this study**
Source: Pozdnyakov et al. (2014)[36]			
254 nm	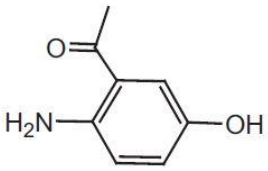 1-(2-amino-5-hydroxyphenyl)ethanone	Shift of the 243 nm peak to a smaller wavelength and a growth in absorbance.	Inconsistent
		No growth of peak near 285 nm.	Inconsistent
		Appearance of a peak near 375 nm.	Inconsistent
266 nm	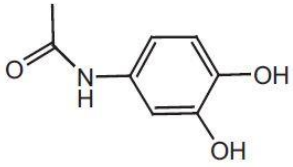 3-hydroxyacetaminophen	Decay of 243 nm peak without a change in the peak location.	Consistent
		Initial increase in peak near 285 nm, then a transition to near uniform decay in absorbance across all wavelengths.	Consistent
		No appearance of peak near 375 nm.	Consistent
282 nm	Multiple primary products listed	Decay of 243 nm peak without a change in the peak location.	Consistent
		No growth of peak near 285 nm.	Inconsistent
		Appearance of a peak near 375 nm.	Inconsistent
Unreacted acetaminophen structure	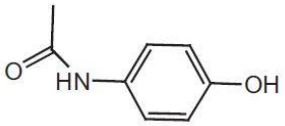		

Referencing Pozdnyakov et al. (2014)[36] shows that 3-hydroxyacetaminophen could be the primary photoproduct of the first phase of the reaction, when there is growth in absorbance near 285 nm. A photoproduct is not given for the second phase of the reaction, when the entire spectrum decays uniformly across all wavelengths. Forte et al. (1984)[46] showed that 3-hydroxyacetaminophen exhibits toxicity in mice, but less than acetaminophen itself. The ecotoxicity of 3-hydroxyacetaminophen is not well studied beyond this.

A total organic carbon (TOC) analysis was conducted to measure if any of the acetaminophen was mineralized to CO_2 during photolysis. A decrease in TOC means mineralization occurred. Two replicate batch trials provided samples for the TOC analysis, each with an initial acetaminophen concentration of 10 ppm. The control samples were not irradiated

with UV light. Data is shown graphically in Figure 11 below. Declining UV-vis absorbance at 243 nm quantifies the disappearance of acetaminophen.

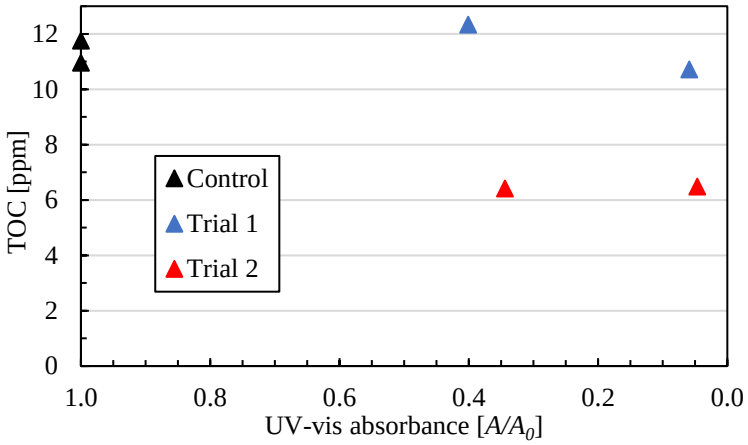

Figure 11: *Total organic carbon analysis of 10 ppm acetaminophen irradiated with 254 nm light. Decreasing UV-vis absorbance at 243 nm indicates the progress of the photolysis reaction.*

TOC changes incongruously with the UV-vis absorbance as the reaction progresses. Sustained TOC presence shows that the primary products of the reaction are organic, albeit some mineralization occurred in Trial 2. The TOC data differed among trials, suggesting experimental error. Three control samples were analyzed but only two are shown in Figure 11. The third sample was measured to contain 77 ppm of TOC and was discarded as erroneous. Such a high level of organic carbon was not possible in the given experimental conditions. The available TOC data shown in Figure 11 suggests that organic species are the primary products of the acetaminophen photolysis.

The batch reaction exhibited time dependent degradation similar to Xu et al. (2018),[32] that also irradiated aqueous acetaminophen with 254 nm light in a batch system. The time dependent absorbance and pseudo-first order logarithmic plots in Xu et al. (2018)[32] are the same shape as in this study, seen below in Figure 12.

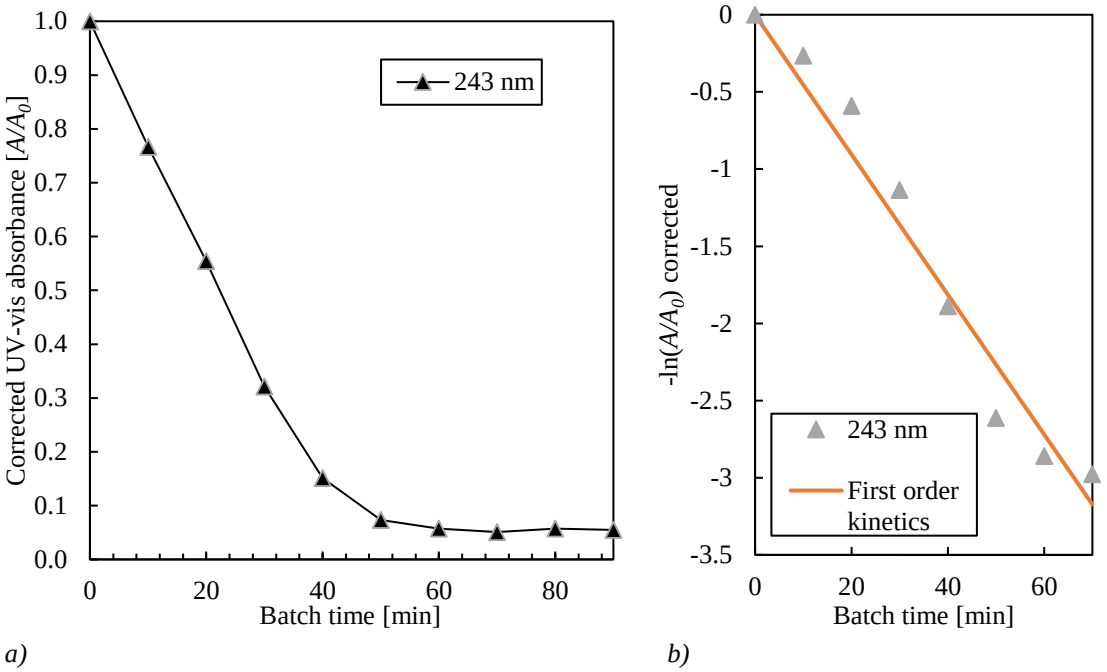

Figure 12: *Kinetic data of batch photolysis. a) Time dependent absorbance data. b) Comparison of data to a pseudo-first order kinetic model with k' = 45.34 x 10^{-3} min^{-1}.*

Absorbance decays in a nearly linear fashion initially. It then transitions to exponential decay before flattening out indefinitely. Data for the first 70 minutes was used to compute *k'*, since the reaction ceases to progress after 70 minutes. A linear fit of -ln(A/A_0) data yields a pseudo-first order rate constant of *k'* = [45.34 ± 4.59] x 10^{-3} min^{-1} (95% confidence). Context is given to the *k'* value by the batch reaction having a fluid depth of 6 mm with a UV light intensity of 23.83 W/m^2 at the surface. The initial concentration was 10 ppm.

Continuous flow photolysis

Acetaminophen photolysis in the 3D printed continuous flow reactor was analyzed with varying flow rate, UV light intensity, and initial concentration. Data is shown graphically in Figure 13 below. UV-vis absorbance at 243 nm determined the amount of acetaminophen degraded. The Beer-Lambert law and data shown in Figure 9 affirm that $C_A/C_{A0} = A/A_0$, where C_A is concentration and A is absorbance. The continuous flow data was compared to ideal MFR and PFR models according to the model definitions in Levenspiel (1999)[38], detailed in Table 3. Pseudo-first order rate constants were calculated for each ideal reactor type using experimental data and are listed in Table 6.

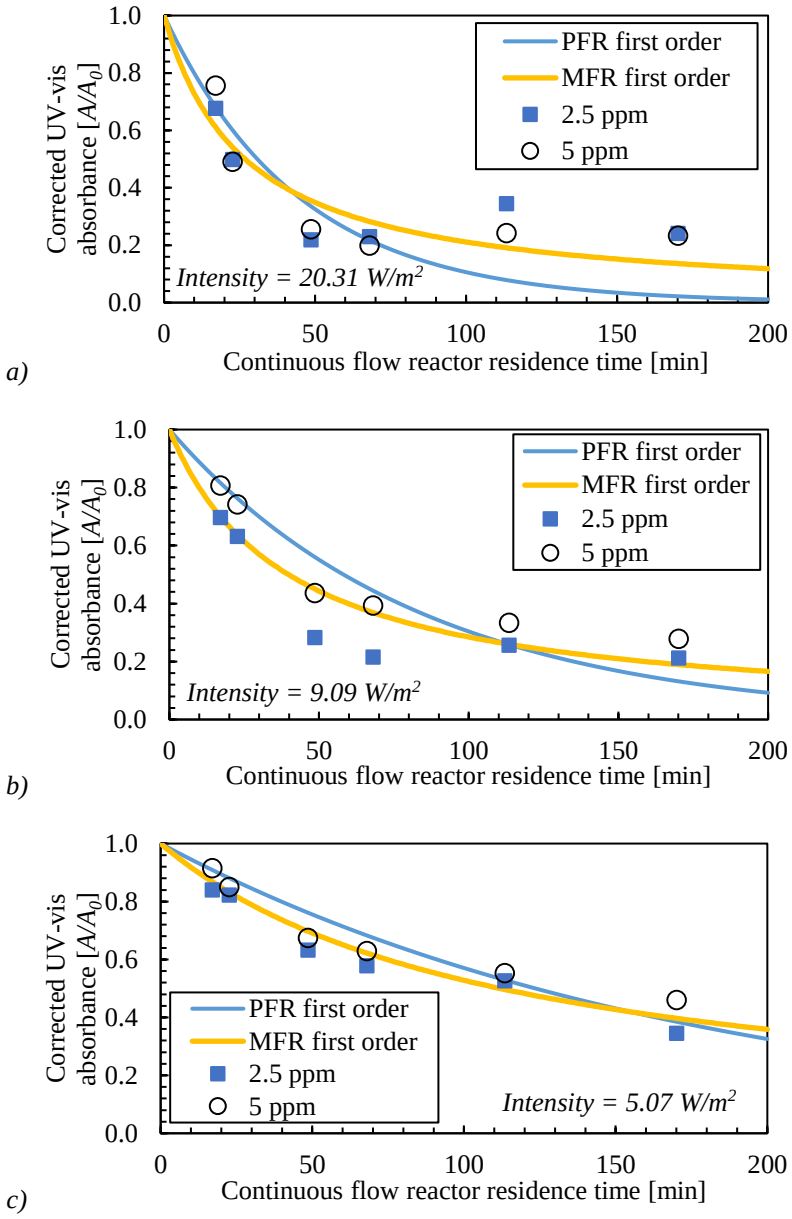

Figure 13: *Acetaminophen photolysis data in continuous flow reactor for UV light intensities of a) 20.31 b) 9.09, and c) 5.07 W/m^2. Inlet acetaminophen concentrations are specified. Idealized reactor models are shown with the best possible fit to the data.*

Acetaminophen photolysis increased with residence time and with light intensity. Consistency in results among inlet acetaminophen concentrations indicates repeatability of the experimental methods. The square error was calculated for each A/A_0 data point in reference to the MFR and PFR models. The pseudo-first order rate constants (k') were manipulated using MS Excel Solver to find the minimum sum of square errors (SSE) for each model and intensity. Minimized SSE statistics for the A/A_0 vs residence time data and model fits are shown below in Figure 14.

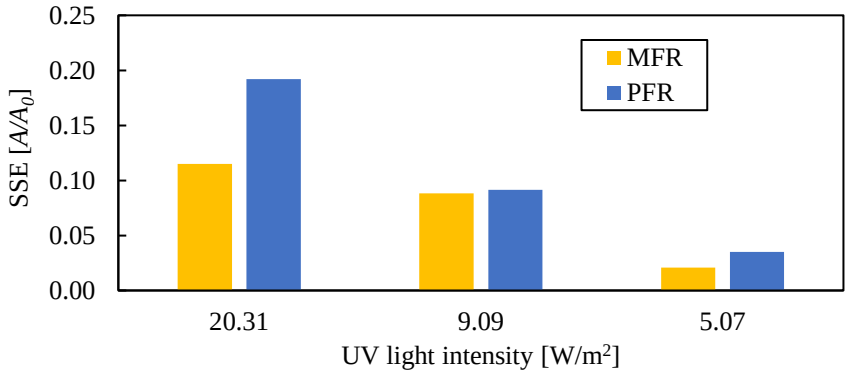

Figure 14: *SSE for ideal reactor model fits to continuous flow absorbance data.*

The pseudo-first order rate constants determined and 95% confidence intervals for *k'* are shown below in Table 6.

Table 6: *Pseudo-first order rate constants for a) MFR and b) PFR models at varied UV light intensities. 95% confidence intervals for k' are reported.*

a)

Mixed flow reactor		
Intensity [W/m^2]	k' x10^3 [min^{-1}]	95% CI x10^3 [min^{-1}]
20.31	37.34	± 22.00
9.09	25.15	± 11.62
5.07	8.94	± 2.27

b)

Plug flow reactor		
Intensity [W/m^2]	k' x10^3 [min^{-1}]	95% CI x10^3 [min^{-1}]
20.31	22.44	± 14.72
9.09	11.92	± 5.33
5.07	5.61	± 1.42

Data aligned closer with performance equations as light intensity decreased, reflected by proportionally narrower confidence intervals. The relationship between UV light intensity and pseudo-first order rate constants was analyzed and is plotted in Figure 15 below.

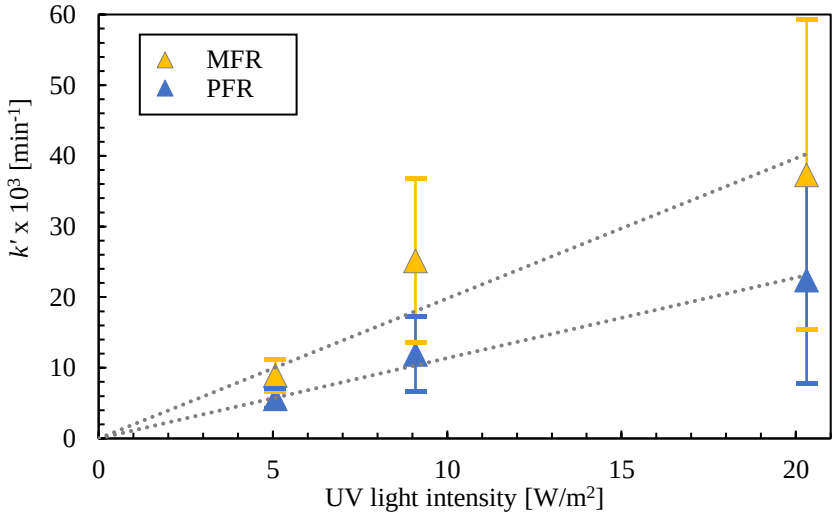

Figure 15: *Relationship between UV light intensity and pseudo-first order rate constant (k') for MFR and PFR reactor models. Dashed lines are a linear fit for each model. Error bars are a 95% confidence interval.*

The rate constants increase with light intensity in a linear fashion. The linear relationship justifies use of a first order approximation to factor light intensity into the reaction rate law. A single rate constant (k) was calculated for each ideal reactor type using data from all intensities. It considered intensity (I) as a first order reactant in the rate law for acetaminophen photolysis, as seen below. The units of k are m^2/W-min and k is related to k' such that $k' = kI$.

$$-r_A = \frac{dC_A}{dt} = k\, I\, C_A$$

MFR and PFR performance equations were then derived with the new rate law and are shown in Table 7 below. The complete derivations are shown in Appendix A: Derivations.

Table 7: *Ideal reactor performance equations considering UV-light intensity for pseudo-first order kinetics*

Idealized reactor model	MFR	PFR
Performance equation for a pseudo-first order reaction considering UV light intensity	$k\,\tau\, I = \frac{X_A}{1-X_A}$	$k\,\tau\, I = \ln\left[\frac{1}{1-X_A}\right]$

Continuous flow A/A_0 data for trials at all UV light intensities was compared to the MFR and PFR models shown in Table 7 above. Residence time and intensity were multiplied to form a single independent variable for kinetic analysis. Figure 16 below shows the absorbance data and ideal reactor model fits.

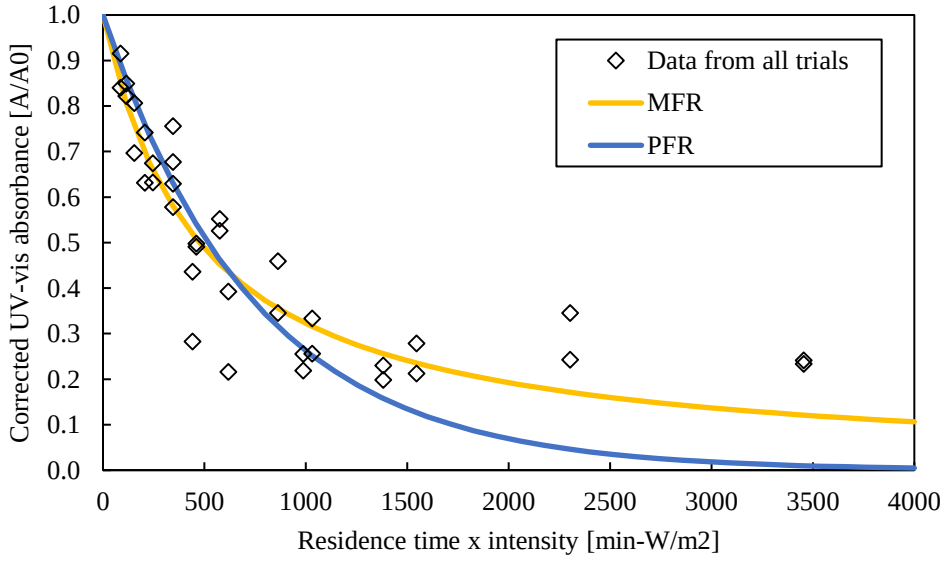

Figure 16: *Acetaminophen photolysis data considering UV light intensity and continuous flow reactor residence time. Idealized reactor models are shown with the best possible fit to the data.*

The same method is used to determine k as was used to determine k'. The k values are manipulated to find the minimum SSEs comparing absorbance data to reactor models. The

pseudo-first order rate constants considering intensity are shown in Table 8, along with 95% confidence intervals for *k* and the SSE for each model fit to A/A_0 data.

Table 8: *Pseudo-first order rate constants for MFR and PFR considering UV light intensity. Confidence intervals are reported along with the SSE for fit of models to UV-vis absorbance data.*

Reactor model	k x10^3	95% CI x10^3	SSE for A/A_0
	[m^2/W-min]		
MFR	2.10	± 0.03	0.291
PFR	1.34	± 0.02	0.519

The *k* values are comparable to literature. Carlson et al. (2015)[33] used a batch reaction with 254 nm light and 50 ppb acetaminophen. An intensity of 1.4 W/m^2 was used and k' = 2.04 x 10^{-3} min^{-1} reported. Diving k' by the intensity yields k = 1.46 x 10^{-3} m^2/W-min, which is between the values reported for MFR and PFR models in this study.

3D printed reactor performance

The continuous flow reactor was designed assuming the 3D printer would replicate CAD models to the exact dimensions specified. Components were designed to fit perfectly together, leaving no room for error in the FDM printing process. The 3D printer actually produced components that were fractions of millimeter larger on all sides than the CAD models. This required manual filing and sanding of most of the components so that the parts would fit together. Leaks were also a significant concern in the reactor. Manual filing and sanding of components destroyed the uniformity of surfaces, allowing for liquid to escape the reactor. Many applications of superglue and silicone caulk were required to make the reactor leak-proof during experimental trials, even at such low flow rates.

The reactor was constructed of PLA, which experienced chemical changes when irradiated with the 254 nm light. A slight yellow discoloration was observed on the top of the reactor after being exposed to the UV light for approximately 10 hours. The discoloration was initially greatest near the center of the top of the reactor. It then became uniform across the reactor top as more trials were completed. The yellow discoloration was the only chemical change observed. It can be seen in Figure 7c near the corners of the reactor top. The UV light source had visible light components that appeared faintly blue, obscuring the yellow discoloration near the center of the reactor top in Figure 7c. The portion of the reactor beneath the exposed acetaminophen did not have a discoloration. There were no unexplained peaks in the UV-vis spectrum that could have been attributed to PLA or a yellow photolysis product leaching into solution. The yellow discoloration affected only the outer surface of the top of the reactor.

Conclusion

Human urine has the potential to be a source of agricultural fertilizer. A problem with urine from the general population is that portions of pharmaceuticals go unmetabolized and exit through urine. Previous studies show that most of these drugs can be taken up by plants when urine is used as fertilizer. Some common pharmaceuticals can make their way into the edible parts of vegetables in significant quantities. Acetaminophen is commonly found in urine and its concentration can be measured with UV-vis spectroscopy. This study characterizes the degradation of aqueous acetaminophen in batch and continuous flow reactions. Photolysis is conducted with UV light at 254 nm without any catalysis or oxidizers, which are used in many other photochemical reactions.

Batch studies confirmed pseudo-first order kinetics in agreement with Xu et al. (2018).[32] UV-vis spectral results for batch trials were compared to Pozdnyakov et al. (2014).[36] The comparison of results suggests 3-hydroxyacetaminophen as a possible product of the reaction in this study. TOC analysis indicates that the products are mostly organic species, by mass.

The continuous flow reactor was uniquely designed, 3D printed, and constructed. Trials showed that more acetaminophen is degraded as residence time and light intensity increase. Continuous flow reactor performance is comparable to MFR and PFR idealized models with respect to residence time. Data corresponds more closely to the ideal reactor models as light intensity decreases. Pseudo-first order rate constants (k') were determined using a best fit of MFR and PFR models to the data at each separate intensity. Rate constants increased linearly with light intensity.

Up to 80% of the acetaminophen was degraded in the experimental conditions of the continuous flow reactor. This demonstrates that levels of the pharmaceutical can be significantly reduced via UV photolysis. The reactor design can be easily scaled up, since the specialized components can be produced quickly with 3D printing. Artificial light sources producing an intense 254 nm wavelength are commonly available on the consumer market. The lack of catalysts and oxidizers reduces costs and eliminates some materials access barriers. The reactor, artificial light, and pump apparatus can be applied quickly and cost-effectively in laboratory or industrial settings. The photolysis data from this study can inform the design of future applications.

Further Research

Scale up of the continuous flow reactor would be limited by the maximum possible size of the glass slide covering the UV light aperture. The slide is made of single crystal sapphire and is a 1-inch square. The vendor used in this study does not have standardized slides larger than 1-inch. Scaling up would require larger slides, numbering up of reactors, or both. Other UV-transparent materials could also be considered, such as fused silica. Other materials may have cost benefits and be more feasible to scale to larger dimensions. Increasing the acetaminophen photolysis would also be aided by a more intense light. This study shows that higher UV light

intensity speeds the rate of degradation. A more intense light, or concentrated light, would give faster photolysis of acetaminophen in the current reactor.

The ideal reactor models for an MFR and PFR were limited in their fit to the data. An MFR assumes perfect mixing within the reactor. A PFR assumes that the reaction progresses as fluid moves unidirectionally in the reactor, and concentration is uniform in the dimension perpendicular to flow. The reactor in this study likely deviates from these assumptions. Computer modeling of the fluid flow within the reactor would go beyond the assumptions of an MFR or PFR. Knowledge of the microfluidics could provide a more accurate kinetic model for photolysis. Designs for scale up and future applications of the reactor would be better informed with a more accurate model of photolysis kinetics.

The products of the acetaminophen photolysis in this study were not directly determined. A possible product is 3-hydroxyacetaminophen, suggested from consistencies with previous studies. Further research would use analytical methods, such as liquid chromatography, to identify and quantify the degradation products from this apparatus. The toxicity of the photoproducts would be of interest. Toxicity would have implication for plants, soil and water microorganisms, and humans that would consume the plants fertilized with urine.

Acetaminophen was the object of this study. Many other drugs are commonly found in urine and are taken up by vegetables when urine is used as fertilizer. Future investigations would gauge the UV photolysis of different drugs in the continuous flow reactor. Drugs like ibuprofen, aspirin, and naproxen are easy to obtain and are found in large quantities in urine. Drugs such as carbamazepine, ciprofloxacin, and erythromycin are also of interest. These compounds are commonly in urine and taken up by vegetables in large proportions, but are not available over the counter. Future studies would compare different pharmaceuticals for their photolysis kinetics and reaction products.

Appendix A: Derivations

Incorporating UV light intensity as a first order approximation for the reaction rate yields the following pseudo-first order rate law:

$$-r_A = \frac{dC_A}{dt} = k\,I\,C_A$$

Starting with the most basic form of the MFR performance equation from Levenspiel (1999)[38]:

$$\tau = \frac{C_{A0} X_A}{-r_A}$$

Adding in the rate law:

$$\tau = \frac{C_{A0} X_A}{k\,I\,C_A}$$

Substituting $C_A/C_{A0} = 1 - X_A$:

$$\tau = \frac{X_A}{k\,I\,(1 - X_A)}$$

Rearranging to produce the MFR performance equation considering UV light intensity:

$$\tau\,I\,k = \frac{X_A}{1 - X_A}$$

Shifting focus to the PFR model and starting with the most basic form of the PFR performance equation from Levenspiel (1999)[38]:

$$\tau = -\int_{C_{A0}}^{C_A} \frac{1}{-r_A}\,dC_A$$

Adding in the rate law:

$$\tau = -\int_{C_{A0}}^{C_A} \frac{1}{k\,I\,C_A}\,dC_A$$

Rearranging and integrating:

$$\tau\,I\,k = -\ln\left[\frac{C_A}{C_{A0}}\right]$$

Substituting $C_A/C_{A0} = 1 - X_A$:

$$\tau\,I\,k = -\ln\left[1 - X_A\right]$$

Simplifying to produce the PFR performance equation considering UV light intensity:

$$\tau\,I\,k = \ln\left[\frac{1}{1 - X_A}\right]$$

Appendix B: Supporting Figures

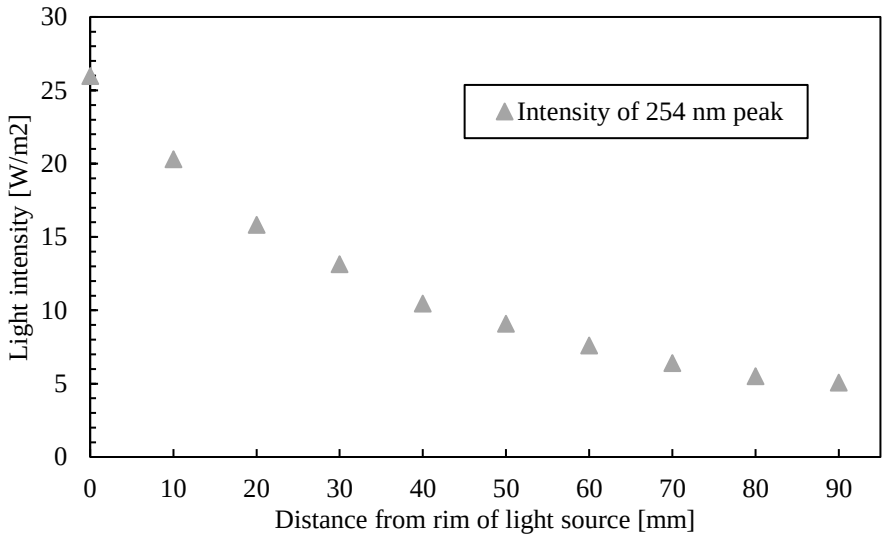

Figure 17: *Relationship between UV light intensity and distance from light source. Light detector was covered with a single crystal sapphire slide to simulate experimental conditions in the continuous flow reactor. Intensity shown is an integration from 251 – 255 nm.*

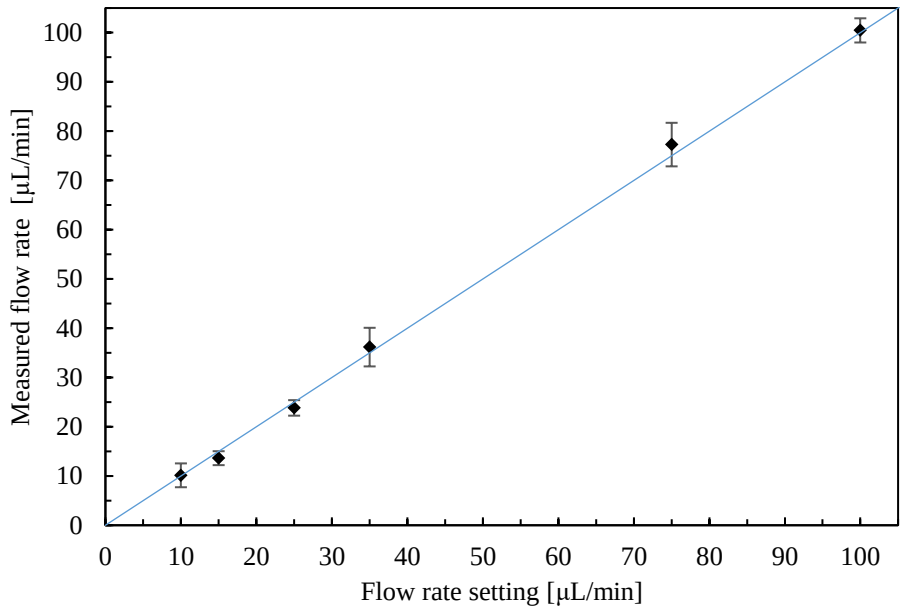

Figure 18: *Calibration curve for syringe pump flow rate. Data points shown are an average of five trials at each flow rate. Error bars represent a 95% confidence interval. The blue line represents exact unity between measured flow and syringe pump flow rate setting.*

References

1. Putnam, D., Composition and Concentrative Properties of Human Urine. Administration, N. A. a. S., Ed. McDonnell Douglas Astronautics Company: Washington, D.C., 1971; pp 38-39.

2. Mihelcic, J. R.; Fry, L. M.; Shaw, R., Global potential of phosphorus recovery from human urine and feces. *Chemosphere* **2011,** *84* (6), 832-839.

3. Smil, V., Phosphorus in the environment: Natural flows and human interferences. *Annual Review of Energy and the Environment* **2000,** *25*, 53-88.

4. Carpenter, S. R.; Bennett, E. M., Reconsideration of the planetary boundary for phosphorus. *Environmental Research Letters* **2011,** *6* (1), 12.

5. Van Vuuren, D. P.; Bouwman, A. F.; Beusen, A. H. W., Phosphorus demand for the 1970-2100 period: A scenario analysis of resource depletion. *Global Environmental Change-Human and Policy Dimensions* **2010,** *20* (3), 428-439.

6. Cordell, D.; Drangert, J. O.; White, S., The story of phosphorus: Global food security and food for thought. *Global Environmental Change-Human and Policy Dimensions* **2009,** *19* (2), 292-305.

7. Manning, D. A. C., How will minerals feed the world in 2050? *Proceedings of the Geologists Association* **2015,** *126* (1), 14-17.

8. Lienert, J.; Gudel, K.; Escher, B. I., Screening method for ecotoxicological hazard assessment of 42 pharmaceuticals considering human metabolism and excretory routes. *Environmental Science & Technology* **2007,** *41* (12), 4471-4478.

9. de Garcia, S. O.; Pinto, G. P.; Encina, P. G.; Mata, R. I., Consumption and occurrence of pharmaceutical and personal care products in the aquatic environment in Spain. *Science of the Total Environment* **2013,** *444*, 451-465.

10. Wu, X. Q.; Conkle, J. L.; Ernst, F.; Gan, J., Treated Wastewater Irrigation: Uptake of Pharmaceutical and Personal Care Products by Common Vegetables under Field Conditions. *Environmental Science & Technology* **2014,** *48* (19), 11286-11293.

11. Winker, M.; Faika, D.; Gulyas, H.; Otterpohl, R., A comparison of human pharmaceutical concentrations in raw municipal wastewater and yellowwater. *Science of the Total Environment* **2008,** *399* (1-3), 96-104.

12. Mullen, R.; Noe-Hays, A.; Nace, K.; Aga, D., Analysis of pharmaceuticals in food crops grown in urine- and struvite-fertilized soil by liquid chromatography tandem mass spectrometry. *Abstracts of Papers of the American Chemical Society* **2015,** *250*, 1.

13. Snyder, S.; Lue-Hing, C.; Cotruvo, J.; Drewes, J. E.; Eaton, A.; Pleus, R. C.; Schlenk, D., Pharmaceuticals in the Water Environment. National Association of Clean Water Agencies, A. o. M. W. A., Ed. American Chemical Society: Washington, DC, 2008.

14. Schwab, B. W.; Hayes, E. P.; Fiori, J. M.; Mastrocco, F. J.; Roden, N. M.; Cragin, D.; Meyerhoff, R. D.; D'Aco, V. J.; Anderson, P. D., Human pharmaceuticals in US surface waters: A human health risk assessment. *Regulatory Toxicology and Pharmacology* **2005,** *42* (3), 296-312.

15. Wu, X. Q.; Ernst, F.; Conkle, J. L.; Gan, J., Comparative uptake and translocation of pharmaceutical and personal care products (PPCPs) by common vegetables. *Environment International* **2013,** *60*, 15-22.

16. Blum, K. M.; Norstrom, S. H.; Golovko, O.; Grabic, R.; Jarhult, J. D.; Koba, O.; Lindstrom, H. S., Removal of 30 active pharmaceutical ingredients in surface water under long-term artificial UV irradiation. *Chemosphere* **2017,** *176*, 175-182.

17. da Silva, J. C. C.; Teodoro, J. A. R.; Afonso, R.; Aquino, S. F.; Augusti, R., Photolysis and photocatalysis of ibuprofen in aqueous medium: characterization of by-products via liquid chromatography coupled to high-resolution mass spectrometry and assessment of their toxicities against Artemia Salina. *Journal of Mass Spectrometry* **2014,** *49* (2), 145-153.

18. Dantas, R. F.; Rossiter, O.; Teixeira, A. K. R.; Simoes, A. S. M.; da Silva, V. L., Direct UV photolysis of propranolol and metronidazole in aqueous solution. *Chemical Engineering Journal* **2010,** *158* (2), 143-147.

19. Dong, H. Y.; Qiang, Z. M.; Lian, J. F.; Qu, J. H., Degradation of nitro-based pharmaceuticals by UV photolysis: Kinetics and simultaneous reduction on halonitromethanes formation potential. *Water Research* **2017,** *119*, 83-90.

20. Pereira, V. J.; Weinberg, H. S.; Linden, K. G.; Singer, P. C., UV degradation kinetics and modeling of pharmaceutical compounds in laboratory grade and surface water via direct and indirect photolysis at 254 nm. *Environmental Science & Technology* **2007,** *41* (5), 1682-1688.

21. Zhang, R. C.; Sun, P. Z.; Boyer, T. H.; Zhao, L.; Huang, C. H., Degradation of Pharmaceuticals and Metabolite in Synthetic Human Urine by UV, UV/H2O2, and UV/PDS. *Environmental Science & Technology* **2015,** *49* (5), 3056-3066.

22. Alharbi, S. K.; Kang, J. G.; Nghiem, L. D.; van de Merwe, J. P.; Leusch, F. D. L.; Price, W. E., Photolysis and UV/H2O2 of diclofenac, sulfamethoxazole, carbamazepine, and trimethoprim: Identification of their major degradation products by ESI-LC-MS and assessment of the toxicity of reaction mixtures. *Process Safety and Environmental Protection* **2017,** *112*, 222-234.

23. Lopes, B. C.; Sanson, A. L.; de Aquino, S. F.; de Souza, C. L.; Chernicharo, C. A. D.; Afonso, R., Behavior of pharmaceuticals in UV photoreactors fed with sewage treated by anaerobic/aerobic system. *Environmental Technology* **2017,** *38* (21), 2775-2784.

24. Luo, S.; Wei, Z. S.; Spinney, R.; Zhang, Z. L.; Dionysiou, D. D.; Gao, L. W.; Chai, L. Y.; Wang, D. H.; Xiao, R. Y., UV direct photolysis of sulfamethoxazole and ibuprofen: An experimental and modelling study. *Journal of Hazardous Materials* **2018,** *343*, 132-139.

25. Nassar, R.; Mokh, S.; Rifai, A.; Chamas, F.; Hoteit, M.; Al Iskandarani, M., Transformation of sulfaquinoxaline by chlorine and UV light in water: kinetics and by-product identification. *Environmental Science and Pollution Research* **2018,** *25* (35), 34863-34872.

26. Reusch, W. Photochemistry. https://www2.chemistry.msu.edu/faculty/reusch/virttxtjml/photchem.htm (accessed 10 April 2019).

27. Reusch, W. Visible and Ultraviolet Spectroscopy. https://www2.chemistry.msu.edu/faculty/reusch/virttxtjml/Spectrpy/UV-Vis/spectrum.htm#uv3 (accessed 10 April 2019).

28. Silbey, R. J.; Alberty, R. A.; Bawendi, M. G., *Physical Chemistry*. Fourth ed.; John Wiley & Sons, Inc.: Hoboken, NJ, 2005; p 944.

29. Gunzler, H.; Williams, A., *Handbook of Analytical Techniques*. First ed.; WILEY-VCH Verlag GmbH: Weinheim (Federal Republic of Germany), 2001; p 1182.

30. 2016 Top Markets Report Pharmaceuticals. Commerce, U. S. D. o., Ed. 2016.

31. Mujahid, A.; Ali, Y.; Afzal, A.; Hussain, T.; Shah, A. T.; Shehzad, K.; Farooq, M. U., Rapid assay of the comparative degradation of acetaminophen in binary and ternary combinations. *Arabian Journal of Chemistry* **2014,** *7* (4), 522-524.

32. Xu, B. J.; Zhan, G.; Xu, B.; Du, H. J.; Luo, H.; Wang, T. F.; Zhan, C. C.; Yang, Y., Degradation of acetaminophen in aqueous solution by UV and UV-activated sludge processes. *Water Science and Technology* **2018,** *78* (10), 2088-2095.

33. Carlson, J. C.; Stefan, M. I.; Parnis, J. M.; Metcalfe, C. D., Direct UV photolysis of selected pharmaceuticals, personal care products and endocrine disruptors in aqueous solution. *Water Research* **2015,** *84*, 350-361.

34. Eskandarian, M. R.; Choi, H.; Fazli, M.; Rasoulifard, M. H., Effect of UV-LED wavelengths on direct photolytic and TiO2 photocatalytic degradation of emerging contaminants in water. *Chemical Engineering Journal* **2016,** *300*, 414-422.

35. Harris, D. C., *Quantitative Chemical Analysis*. Ninth ed.; W. H. Freeman and Company: New York, NY, 2016; p 792.

36. Pozdnyakov, I. P.; Zhang, X.; Maksimova, T. A.; Yanshole, V. V.; Wu, F.; Grivin, V. P.; Plyusnin, V. F., Wavelength-dependent photochemistry of acetaminophen in aqueous solutions. *Journal of Photochemistry and Photobiology a-Chemistry* **2014,** *274*, 117-123.

37. Martignac, M.; Oliveros, E.; Maurette, M. T.; Claparols, C.; Benoit-Marquie, F., Mechanistic pathways of the photolysis of paracetamol in aqueous solution: an example of photo-Fries rearrangement. *Photochemical & Photobiological Sciences* **2013,** *12* (3), 527-535.

38. Levenspiel, O., *Chemical Reaction Engineering*. Third ed.; John Wiley & Sons, Inc.: New York, NY, 1999; p 668.

39. Kawabata, K.; Sugihara, K.; Sanoh, S.; Kitamura, S.; Ohta, S., Ultraviolet-photoproduct of acetaminophen: Structure determination and evaluation of ecotoxicological effect. *Journal of Photochemistry and Photobiology a-Chemistry* **2012,** *249*, 29-35.

40. Kawabata, K.; Sugihara, K.; Sanoh, S.; Kitamura, S.; Ohta, S., Photodegradation of pharmaceuticals in the aquatic environment by sunlight and UV-A, -B and -C irradiation. *Journal of Toxicological Sciences* **2013,** *38* (2), 215-223.

41. Stansbury, J. W.; Idacavage, M. J., 3D printing with polymers: Challenges among expanding options and opportunities. *Dental Materials* **2016,** *32* (1), 54-64.

42. Wang, X.; Jiang, M.; Zhou, Z. W.; Gou, J. H.; Hui, D., 3D printing of polymer matrix composites: A review and prospective. *Composites Part B-Engineering* **2017,** *110*, 442-458.

43. Stefanov, B. I.; Lebrun, D.; Mattsson, A.; Granqvist, C. G.; Osterlund, L., Demonstrating Online Monitoring of Air Pollutant Photodegradation in a 3D Printed Gas-Phase Photocatalysis Reactor. *Journal of Chemical Education* **2015,** *92* (4), 678-682.

44. Lopes, M. G. M.; Santana, H. S.; Andolphato, V. F.; Russo, F. N.; Silva, J. L.; Taranto, O. P., 3D printed micro-chemical plant for biodiesel synthesis in millireactors. *Energy Conversion and Management* **2019,** *184*, 475-487.

45. Zhao, F.; Cambie, D.; Janse, J.; Wieland, E. W.; Kuijpers, K. P. L.; Hessel, V.; Debije, M. G.; Noel, T., Scale-up of a Luminescent Solar Concentrator-Based Photomicroreactor via Numbering-up. *Acs Sustainable Chemistry & Engineering* **2018,** *6* (1), 422-429.

46. Forte, A. J.; Wilson, J. M.; Slattery, J. T.; Nelson, S. D., THE FORMATION AND TOXICITY OF CATECHOL METABOLITES OF ACETAMINOPHEN IN MICE. *Drug Metabolism and Disposition* **1984,** *12* (4), 484-491.